

# Application of Hydrodynamic Simulation and Frequency Analysis for Assessment of Sediment Deposition and Vegetation Impacts on Floodplain Inundation

Tomasz Dysarz\*, Joanna Wicher-Dysarz

Department of Water and Sanitary Engineering, Poznań University of Environmental and Life Sciences,  
Piątkowska 94A, 60-649 Poznań, Poland

*Received: 9 November 2010*

*Accepted: 27 May 2011*

## Abstract

The problem analyzed in our paper is quantification of the impact of sediment deposition and riparian vegetation growth on floodplain inundation frequency. An additional factor is water reservoir operation. A Warta River reach was selected for the study. This natural channel is located above the Jeziorsko Reservoir. The applied methodology is a combination of data collection, hydrodynamic model simulations, and analysis of water stage frequencies. Computations and analyses showed interesting relations between elements of the river system studied. Floodplain inundation frequency was found permanently increasing. Although the main factor responsible for this is sediment deposition, the influence of riparian vegetation is important at higher water stages.

**Keywords:** flooding frequency, hydrodynamic simulation, sediment and vegetation impacts, reservoir performance

## Introduction

The main problem we investigated here is the impact of long-term river processes on hydraulic conditions in the water channel and floodplain. The processes are sediment accumulation and riparian vegetation growth. In our study the changes are not natural, but are induced by the operation of the reservoir located downstream. The method used to quantitatively assess their impact is a combination of field data collection, hydrodynamic simulation, and analysis of simulation results. The central point of the methodology applied is analysis of water stage frequency curves. The analyzed changes in flooding frequency are responsible for ecosystem development and the risk of a backwater dike break in the inlet part of the reservoir.

For the purpose of the current study in Poland, a Warta River reach above Jeziorsko Reservoir was chosen. The intensive water management in the reservoir decreased the flow rates in the Warta River, thus inducing sediment deposition in the inlet. This process affected the channel capacity and hydraulic conditions. Another process considered is growth of riparian vegetation in the river floodplains. The vegetation directly affects floodplain roughness and capacity. Hence, there are three processes influencing the flooding frequency in the backwater part of the Warta River. These are:

- (i) reservoir performance
- (ii) sediment deposition
- (iii) vegetation growth

In this paper we analyze the effects of these three processes. Analysis of water stage frequencies enables comparison and presentation of results in more quantitative form.

---

\*e-mail: dysarz@up.poznan.pl

The problems studied here have been intensively investigated over the last decades, mainly because of their importance for water management, regional economy, and human safety. Exemplary relations between the hydrological regime and the riparian vegetation dynamics was given in [1]. The Authors linked the annual average depth in the river floodplains and average diameter of trees growing in the area studied. In [2] the riparian wetland vegetation dynamics was analyzed in relation to the flow changes and sediment accumulation. The relations between the river hydrologic regime and riparian vegetation were studied in [3]. Similar research presented in [4] resulted in formulation of basic principles and consequences of water regime changes.

The changes in the hydraulic conditions in a river may be induced by many different factors, including anthropogenic, as well as natural processes. However, one of the most important anthropogenic impacts is damming of the river, as shown in [5]. The hydraulic and hydrologic changes linked to degradation of river ecosystems located below the dams have been studied by many authors, e.g. [6-8]. Dam impact on the upstream condition has also been intensively investigated (e.g. [9, 10]). In [9] it was proved that dams totally changed the hydraulic and ecological conditions along the Kafue River reach (Zambia) by almost permanent inundation of floodplains. In the second paper [10], the Authors analyzed the relation between flood magnitude changes and water management of a dam, river engineering, and climate change impacts.

Many methods have been proposed for assessment of hydraulic and hydrologic changes, including simple ones like equal discharge measurements [10] and complex analyses constructed on the basis of discharges and water table frequency [6, 7, 11, 12]. Mathematical models have been often applied for simulation of water system behavior e.g. [6, 13]. In each case, the methodology applied should match the specific features of the system studied and processes occurring there, as well as data availability.

The main aim of our paper is to test the application of simulated frequency curves for assessing sediment deposition and vegetation growth impact on hydraulic conditions in a river and its floodplains. The term "simulated" is used here to indicate that the used frequency curves are not the results of observations and/or measurements, but the results of computation. However, the field data were used to configure the hydrodynamic simulation model reconstructing the hydraulic conditions in the river.

## Materials and Methods

### Description of the Study Site

The Warta River is the third longest river in Poland, just after the Vistula and Oder rivers. The Warta's length is 808.2 km and total catchment area is 54,528.7 km<sup>2</sup>. Flood risk in the Warta is great. During more than 150 years of observation, the emergency water stage in the Sieradz gauge station has been exceeded 145 times.

Damaging floods have occurred over 40 times. The largest flows were observed in 1997 and 2010, when disastrous floods affected all of Poland.

One of the most interesting objects in the Warta River is Jeziorsko Reservoir (Fig. 1). Jeziorsko dam is located at km 484+300 and the inlet part of the reservoir is between km 500 and km 502 (Fig. 2). The measurements and observations in the Sieradz gauge station (km 521+000) are the most relevant to assess the natural conditions in the area under investigation. This gauge station is located upstream of the reservoir at such a distance that the influence of a dam operation can be neglected. During the periods analyzed (1963-70, 1973-83, 1993-95, and 1997-2001), the average discharge observed was 51.94 m<sup>3</sup>/s (absolute average), but it varied from 10 m<sup>3</sup>/s (absolute minimum) to 440 m<sup>3</sup>/s (absolute maximum).

The Jeziorsko reservoir was built in 1986. For the first time it was filled up to the admissible maximum water level (121.5 m a.s.l.) in 1991. The hydro-power plant was put into operation in 1995. The admissible minimum and maximum water levels in the reservoir are 116.0 m a.s.l. and 121.5 m a.s.l., respectively. From the very beginning the reservoir offered good conditions for water birds in the upper part. In 1998 the Ministry for Environmental Protection established a nature reserve in the upper part of the reservoir (Fig. 2). According to The Polish Environmental Protection Act (1998), river engineering actions are not allowed in the reservoir.

The river reach profile under investigation is shown in Fig. 2. There are two measured bottom profiles and three simulated water tables. The first bottom is the effect of river regulation before the construction of Jeziosko Dam.

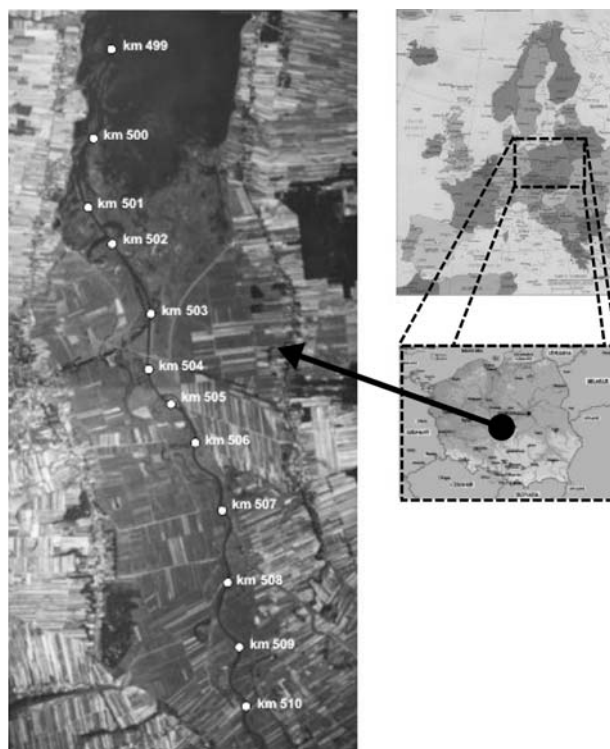


Fig. 1. Location of Jeziorsko Reservoir (right) and its inlet (left).

These data are marked as “bottom 1985.” The second geometry is the result of the field measurements made in 2004 (“bottom 2004”). The water tables shown in Fig. 2 are the results of simulation with the help of HEC-RAS package. More details about HEC-RAS could be found in the following sub-sections. The simulations are performed for the maximum observed discharge of 440 m<sup>3</sup>/s. The flow is computed for two profiles and three different boundary conditions in the following combination:

- (i) free outflow, no reservoir over bottom 1985
- (ii) minimum admissible water level in the reservoir over bottom 2004
- (iii) maximum admissible water level in the reservoir over bottom 2004

Some of the river system elements are presented in Fig. 2 along the river reach profile. The Jeziorsko reservoir is located downstream of the river. The bridge in the town of Warta is treated as the reference cross-section located above the reservoir. The Sieradz gauge station is located upstream. The river reach under investigation is located between the bridge in the town and the reservoir. This is where the Jeziorsko nature reserve was established.

The results shown in Fig. 2 indicate an increase in water stages in the area under investigation. This is the effect of three processes mentioned in the Introduction. In 1998 the results of field measurements along the river reach from Km 494+330 to Km 520+850 confirmed a significant sediment deposition and decrease in the water surface slope [14]. Such changes increase the flood risk related to dike breach by overtopping. It is supposed that this kind of risk is continuously increasing with the vegetation succession. This problem was indicated by local researchers (e.g. [14]).

### Field Measurements and Data Collection

The set of available data consists of:

- (a) system geometry
- (b) discharges and water stages in the system
- (c) state of vegetation cover

The channel and floodplain elevations have been observed for a long period of time in the area under consideration. The most basic set of data comes from the river regulation design prepared in 1975 [14]. The regulated river seemed to be stable and it was not subject to any changes until the reservoir was open between 1986 and 1991.

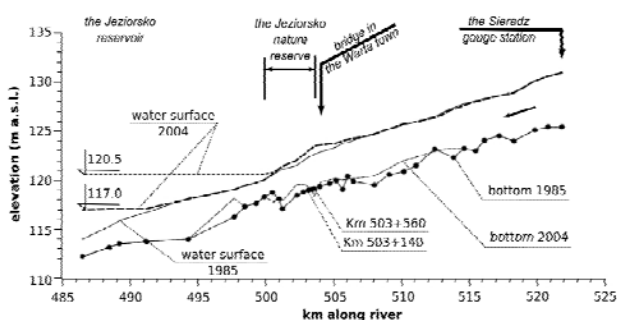


Fig. 2. Simulated water surface profile for maximum observed discharge at Sieradz gauge station (WWQ = 440 m<sup>3</sup>/s).

Hence, this set of data may be considered as the original terrain and river bottom from 1985 without any significant influence of the processes analyzed. The other sets of data considered are the measurements made in 1997 and 2004 [14]. Hence, the system geometry data consists of three sets of river bottom and floodplain measurements in 37 cross-sections covering the river reach from the Sieradz gauge station (Km 520+850) to the Jeziorsko dam (Km 486+500). These data were used to construct three stages of the river bottom and floodplain evolution.

The other data used in our analyses are:

- (1) discharges and water stages observed in the Sieradz gauge station
- (2) water levels measured at the Jeziorsko Dam headwaters

The set of data from the Sieradz gauge station consists of daily measurements from the periods 1963-70, 1973-83, 1993-95, and 1997-2001, so over 27 years. The data collected from the Sieradz gauge station are used as scenarios of inflows to the river system analyzed. The main assumption is that hydraulic conditions in the Sieradz gauge station are not affected by the processes investigated. The water stages at Jeziorsko headwater were observed during the period of reservoir performance, from 1992 to 2001. The data were used to design the typical scenario of reservoir performance along the year.

The impact of vegetation on flow resistance was assessed on the basis of measurements and empirical formulae. The relationship between Manning's roughness coefficient and vegetation characteristics was constructed. The basis for this relationship were the results shown in [15]. The problem is described in following sub-sections. The vegetation characteristics are expressed as bush density and average stalk diameter. Necessary measurements were made and published in [16].

### Hydrodynamic Model

For the simulation of the river flow, the classical HEC-RAS package was implemented. The software was developed at the Hydrologic Engineering Center, part of the U.S. Corps of Engineers (<http://www.hec.usace.army.mil/>). The most important elements of the package are hydrodynamic models for steady and unsteady flow simulation [17]. The primary basis of the unsteady flow model is a well known set of St. Venant equations. The equations are approximated numerically by means of the finite difference method. The fundamental principles and procedures for such an approach have been described in [18-20]. The particular equations, in the form implemented in the HEC-RAS, were explained in [21]. The difference from the classical St. Venant system is the extension for cases including meandering rivers with broad floodplains. The complete description of the approaches and methods applied in the HEC-RAS package was presented in [17].

The HEC-RAS package has been tested and used successfully in many cases (e.g. [6]). Hence, the model may be applied to solve the problem described. Close relation of the model structure to the physical conservation laws is a great

advantage. This feature enables proper validation of simulation results on the basis of accurate field measurement data. The HEC-RAS model was configured in such a way that the system geometry corresponded to the four stages of the river bottom evolution. The first analyzed state of the system was the primary regulated bottom [14]. This geometry was considered as the pre-dam condition coming from 1985. It was also assumed to describe the river system state at the beginning of the reservoir operation. The second geometry was prepared on the basis of measurements made in 1997 [14]. This stage of the system corresponded to the river state a few years after the reservoir opening. It was assumed that the vegetation cover changes in the period 1985-97 were so slight that their effect could be neglected. Hence, the roughness in the particular cross-sections was the same in 1985 and 1997. The third geometry of the system was prepared on the basis of measurements made in 2004 and corresponded to the most recently observed conditions. However, the third scheme does not reflect the roughness changes caused by vegetation growth. This element is included in the fourth system geometry. The method used is described below. The current state of the system may be assessed in two ways: with and without vegetation growth.

The riparian vegetation impact on the flow conditions may be modeled as changes in Manning's roughness coefficients  $n$ . However, these coefficients depend on vegetation characteristics as well as water depth presents [15] the formula describing the flow rate changes in the channel. The formula was developed for a channel with non-submerged vegetation in steady flow conditions:

$$u = \sqrt{\frac{2gi_0}{C_w md}} \quad (1)$$

...where  $g$  is the acceleration of gravity and  $i_0$  is the bottom slope. The parameters  $C_w$ ,  $m$ , and  $d$  characterize riparian vegetation:  $C_w$  is the coefficient reflecting seasonal changes in leaf cover, its values were taken as  $C_w = 1.05$  for winter period and  $C_w = 1.40$  for summer [22];  $m$  is the average number of bushes in one square meter; and  $d$  is the average diameter of bush stalks.

Following this concept and applying Manning's equation for the wide channel, the formula for the roughness coefficient can be derived:

$$n = h^{2/3} \sqrt{C_w \frac{md}{2g}} \quad (2)$$

...where  $n$  is Manning's roughness coefficient and  $h$  is depth. The presented approach was used to describe the changes in roughness of the floodplain. Parameters  $m$  and  $d$  were determined on the basis of measurements made in 2004 and 2005 [16].

Hydro-morphological stages of the system's evolution are presented as five potential river states:

(1) The bottom corresponding to pre-dam conditions (1985) with free outflow in the outlet (denoted as 1985-a or "the first state")

- (2) The bottom corresponding to pre-dam conditions (1985) with outflow corresponding to the average annual scheme of reservoir operation (1985-b)
- (3) The bottom measured in 1997, but with the initial roughness and outflow as above (1997)
- (4) The bottom measured in 2004, but with the initial roughness and outflow as above (2004-a)
- (5) The bottom measured in 2004 with roughness reflecting the current state of vegetation and its seasonal variation, outflow corresponding to the average annual scheme of reservoir operation (2004-b, "final state")

The configuration of the unsteady flow module in the HEC-RAS package is completed by proper boundary conditions. The flow data collected from the Sieradz gauge station are imposed as upstream discharge hydrographs. The outflow conditions consist of typical water stage hydrograph constructed on the basis of measurements from the Jeziorsko dam headwater.

Twenty-seven simulations for each of the five stages of the hydro-morphological conditions in the river were performed. The computational time step is chosen as 15 minutes to preserve stability of computations. Despite this, only the results produced for each day at 7 a.m. were analyzed. This approach corresponds to the procedures of river stage observations in Poland, and it was used to maintain the data homogeneity for possible comparative studies.

### Analysis of Water Stages Frequency

The obtained results were processed by means of frequency analysis. The basic relative frequency curves for the cross-sections in the area considered were prepared. The definition of relative frequencies is adopted from [23]. The relative frequency  $f_s(H)$  of water stages is computed as follows:

$$f_s(H_i) = \frac{n_i}{N} \quad (3)$$

...where  $N$  is the total number of results analyzed and  $n_i$  is the number of such results that  $H_i - \Delta H < H < H_i$ . Length  $\Delta H$  is selected for each analyzed cross-section in such a way that the total interval of water stages variation is divided into 50 sub-intervals.

For the sake of clarity the Pearson type III probability density curve is fitted to the results for the first state (1985-a) at each cross-section analyzed. The method of moments [23] is used to fit distribution to the results.

### Relation between Elements of the Method Applied

Flooding frequency is expressed here as the frequency of potential inundation of floodplains. It is defined by relative frequencies from equation (3) as follows:

$$FFI = \sum_{H_i > H_b} f_s(H_i) \quad (4)$$

...where  $FFI$  is the frequency of floodplain inundation and  $H_b$  is the elevation of floodplain bottom.  $FFI$  is a specific

value characterizing each state of the river system defined in the previous sub-section.

In this sense the frequency depends on the system inflows and outflows, and the system's parameters. The first element is represented by discharge hydrographs observed. The measurements were made at the gauge station and were not affected by changes in the river reach investigated. The typical water stage hydrographs influenced by the dam and hydro-power plant operation are the second element. The third element is made of the system's parameters describing the hydraulic transport abilities in the reach. Changes in the third element make the system non-stationary. This means that the system is more complex for investigation, taking into account any long-term effects. The non-stationarity of the system analyzed is related to the processes directly inducing changes in hydrologic measures, such as reservoir operation, sediment deposition and vegetation growth.

Fig. 3 shows the relationships between the elements of the method applied. The external impacts are understood as elements of the system, which are not affected by changes in the river reach. The data describing the evolution of the reach are included in the rectangle denoted as non-stationary elements. It is divided into two groups, namely river bed changes and roughness changes. The first set of data is used to prepare five states of the river system listed above. The second is applied in the configuration of final state (2004-b) according to equation (2).

To distinguish the importance of particular factors influencing the frequency of floodplain inundation, two measures are defined:

- the increase in frequency between two river states related to the total increase in flooding frequency:

$$\Delta FFI_j^{(1)} = \frac{FFI_j - FFI_{j-1}}{FFI_{2004b} - FFI_{1985a}} \cdot 100 \quad [\%] \quad (5)$$

- the increase in frequency between two river states related to the initial flooding frequency:

$$\Delta FFI_j^{(2)} = \frac{FFI_j - FFI_{j-1}}{FFI_{1985a}} \cdot 100 \quad [\%] \quad (6)$$

The measures may be determined for each cross-section analyzed. The subscripts denote the river state. Symbol *j* stands for 1985-b, 1997, 2004-a, 2004-b. Hence, four values can be calculated in a cross-section for each measure.

### Simplified Assessment of Uncertainty

One of the most important problems with the models applied and reliability of the methodology presented is the uncertainty linked to inaccuracies of parameter estimation. This subject is strongly related to model sensitivity. The methods used are described in a number of books and papers, e.g. [24]. Generally, there are sophisticated and time-consuming techniques that enable detailed evaluation of uncertainty sources. Some of these methods were applied in flow problems in the past, e.g. [25]. Analysis of uncertainty should be made taking into account the purpose and capacity of the paper. Hence, we decided just to illustrate the problem. This is the reason why a number of simplifying assumptions have been introduced. The assumptions are presented below.

In the presented analysis only the main source of uncertainty is taken into account, namely the inaccuracy of roughness coefficient *n*. It is assumed that the uncertainty related to the frequency of floodplain inundation *FFI* is analyzed. The analysis is limited to the only one cross-section located at km 503+560. The number of river system states is also reduced for this analysis. We focus on the uncertainty of flooding frequency in the state 2004-a. The number of roughness coefficients used in the simulations is huge. Hence, the analysis applied here is limited to the influence of three selected coefficients. These are the coefficients determined for channel in cross-sections 503+560 (the same as used for frequency analysis), 513+490 (cross-section upstream), and 494+330 (downstream).

The roughness coefficient values were determined on the basis of the tables shown in [26]. The range of roughness coefficient variability for the channel in the investigated Warta River reach was [0.025, 0.055] in s·m<sup>-1/3</sup>. Because there is no valid information about probability distribution

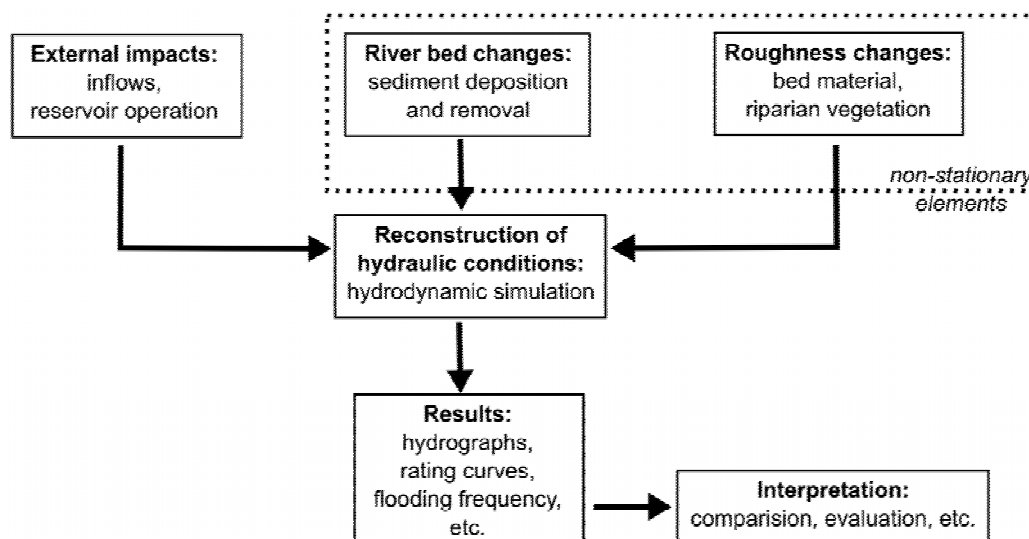


Fig. 3. Graphical representation of relationships between the elements of the method applied.

function over that range, uniform distribution was chosen. Hence, the expected value of the roughness coefficient is  $0.040 \text{ s}\cdot\text{m}^{-1/3}$  and its standard deviation is  $0.009 \text{ s}\cdot\text{m}^{-1/3}$ . The accuracy of roughness coefficient determination in technical problems is equal to  $\pm 0.001 \text{ s}\cdot\text{m}^{-1/3}$ , meaning that the continuous range  $[0.025, 0.055]$  may be approximated by a discrete set of values in the form  $\{0.025, 0.026, \dots, 0.055\}$ . The calculations were made for 15 values picked up from this set. The simulation was repeated for each value and the frequency of floodplain inundation (*FFI*) in cross-section 503+560 was determined. Such analyses enabled estimation of parameters characterizing the flooding frequency variability. These are: expected value of frequency  $E_f$ , standard deviation  $\sigma_f$ , lower  $FFI_m$ , and upper  $FFI_M$  bounds.

Next, a comparison of the estimated characteristics with the frequency obtained in the primary simulation was made. The following measures were used:

- relative difference between the obtained and expected frequency of floodplain inundation

$$RDF = \frac{|FFI - E_f|}{FFI} \cdot 100 \quad [\%] \quad (7)$$

- relative width of frequency range

$$RWF = \frac{|FFI_M - FFI_m|}{FFI} \cdot 100 \quad [\%] \quad (8)$$

In addition, selected values are presented in scatter plot according to the description of the scatter plot given in [24].

## Results

### Simulation Results

The simulation results for four cross-sections from the area denoted as the Jeziorsko nature reserve in Fig. 2 were

analyzed. The cross-sections are located at Km 503+560, Km 503+380, Km 503+140, and Km 502+800. Two of them are marked in Fig. 2. The most basic results are the frequency curves of water stages for the cross-sections at Km 503+560 and Km 503+140 (Fig. 4). The results for the first state (1985-a) are presented as Pearson III curve (black continuous lines). The results for the final state (2004-b) are presented in non-smoothed form (grey bars). In addition, the floodplain elevations and elevations of dike crest are marked in Fig. 4 (black dashed lines).

The other results presented in Tables 1-4 are the characteristic values representing parameters and hydraulic conditions in the analyzed cross-sections for each of the river states. The basic values in the tables are the floodplain and dike crest elevations, average water stage, its standard deviation and frequency of floodplain inundation. In addition, there are also frequencies of exceedance determined for particular stages. The stages chosen are elevations below dike crest in 0.5 m, 1.0 m, and 1.5 m. These results are presented for sections at Km 503+560 (Table 1) and Km 503+380 (Table 3).

The results are also presented in Fig. 5 showing changes in the floodplain inundation frequency across years. The results are shown for the cross-sections at Km 503+560 and Km 503+140. Particular states are denoted as dots or rectangles. Shadows are used to indicate the impacts of sediment accumulation and vegetation succession.

### Comparison of Impacts

The importance of particular processes for the frequency of floodplain inundation is assessed for two cross-sections located in km 503+560 and 503+140. The results are shown in Tables 5-6 and Fig. 6. The tables include the frequency of floodplain inundation *FFI*, the increase in *FFI* between river states and two measures defined by formulae (5) and (6). The values of frequencies and measures are calculated for particular river states. The last column denoted

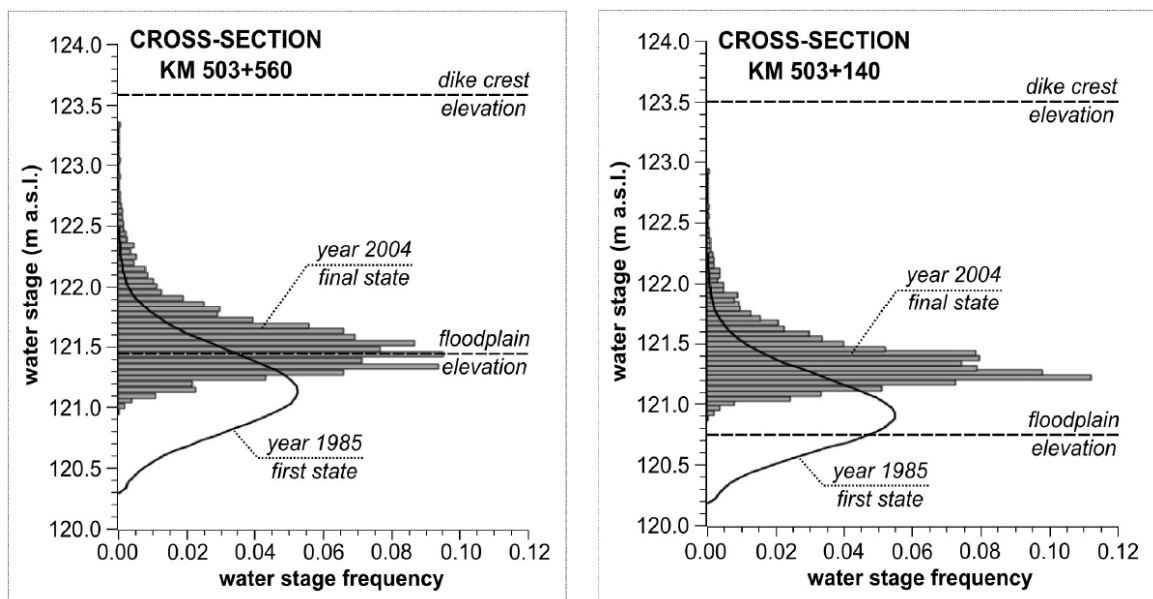


Fig. 4. Water stage frequencies simulated for the cross-section at km 503+560 and km 503+140 in the first and final states of the river channel.

Table 1. Basic results for the cross-section at km 503+560.

State	1985-a (first state)	1985-b	1997	2004-a	2004-b (final state)
floodplain elevation (m a.s.l.)	121.45				
dike crest elevation (m a.s.l.)	123.59				
average water stage (m a.s.l.)	121.14	121.16	121.35	121.46	121.52
standard deviation of water stages (m)	0.34	0.32	0.22	0.21	0.26
frequency of floodplain inundation – symbol <i>FFI</i>	0.197	0.191	0.267	0.485	0.572
frequency of inundation in 0.5 m below dike crest	0.000				<b>3.00 x 10<sup>-04</sup></b>
frequency of inundation in 1.0 m below dike crest	0.000				<b>3.33 x 10<sup>-03</sup></b>
frequency of inundation in 1.5 m below dike crest	0.000				<b>3.59 x 10<sup>-02</sup></b>

Table 2. Basic results for the cross-section at km 503+380.

State	1985-a (first state)	1985-b	1997	2004-a	2004-b (final state)
floodplain elevation (m a.s.l.)	120.96				
dike crest elevation (m a.s.l.)	123.50				
average water stage (m a.s.l.)	121.07	121.09	121.30	121.42	121.48
standard deviation of water stages (m)	0.32	0.30	0.20	0.19	0.25
frequency of floodplain inundation – symbol <i>FFI</i>	0.594	0.662	0.990	0.998	1.000
frequency of inundation in 0.5 m below dike crest	0.000				<b>3.00 x 10<sup>-04</sup></b>
frequency of inundation in 1.0 m below dike crest	0.000				<b>3.00 x 10<sup>-04</sup></b>
frequency of inundation in 1.5 m below dike crest	0.000				<b>3.00 x 10<sup>-04</sup></b>

Table 3. Basic results for cross-section in km 503+140.

State	1985-a (first state)	1985-b	1997	2004-a	2004-b (final state)
floodplain elevation (m a.s.l.)	120.75				
dike crest elevation (m a.s.l.)	123.51				
average water stage (m a.s.l.)	120.94	120.96	121.23	121.31	121.35
standard deviation of water stages (m)	0.30	0.29	0.19	0.18	0.23
frequency of floodplain inundation – symbol <i>FFI</i>	0.692	0.772	1.000		

as “TOTAL” includes final or total values. The final value is given for *FFI*. The increase in *FFI* is summarized. The total value is also given for  $\Delta FFI_j^{(1)}$ .

Table 5 includes results for the cross-section in km 503+560. Some of them are confusing. It was noted that the frequency of floodplain inundation *FFI* decreases for state 1985-b. Supposedly, the impact of the reservoir is so small in this cross-section that the values obtained are prone to numerical errors. Such problems were not encountered for the cross-section 503+140 shown in Table 6.

Some of the results also are presented in Fig. 6. These are  $\Delta FFI_j^{(1)}$  values for the same cross-sections as those described in Tables 5 and 6. The measure indicate the impacts of particular processes. The processes are as follows:

- reservoir operation marked as “reservoir”
- sediment deposition during 1985-1997 denoted as “sediment (1)”
- sediment deposition during 1997-2004 denoted as “sediment (2)”
- vegetation succession denoted as “vegetation”

Table 4. Basic results for cross-section in km 502+800.

State	1985-a (first state)	1985-b	1997	2004-a	2004-b (final state)
floodplain elevation (m a.s.l.)	120.70				
dike crest elevation (m a.s.l.)	123.52				
average water stage (m a.s.l.)	120.74	120.78	121.11	121.21	121.22
standard deviation of water stages (m)	0.27	0.26	0.15	0.16	0.20
frequency of floodplain inundation – symbol <i>FFI</i>	0.553	0.627	1.000		

Table 5. Measures of increase in frequency of floodplain inundation for the cross-section at km 503+560.

State	1985-a (first state)	1985-b	1997	2004-a	2004-b (final state)	TOTAL
$FFI_j$	0.197	0.191	0.267	0.485	0.572	0.572
$FFI_j - FFI_{j-1}$	-	0*	0.070	0.218	0.087	0.375
$\Delta FFI_j^{(1)}$	-	0%*	18.7%	58.1%	23.2%	100%
$\Delta FFI_j^{(2)}$	-	0%*	35.5%	110.7%	44.2%	-

\*confusing results interpreted as oscillations around zero increase

### Assessment of Uncertainty

The results of uncertainty assessment are shown in Table 7 and Fig. 7. Table 7 give a summary of parameters described in the previous section of this paper. The columns show the symbols of parameter and values obtained for each cross-section analyzed in the uncertainty assessment. The first row contains values of roughness coefficient  $n$  used in the basic simulation. In the second row, the primary value of flooding frequency  $FFI$  is presented. Next rows show estimation of expected frequency  $E_f$ , standard deviation  $\sigma_f$ , lower  $FFI_m$  and upper  $FFI_M$  bounds of frequency. There are also measures of uncertainty defined by formulae (6) and (7) in the last two rows,  $RDF$  and  $RWF$ , respectively.

Fig. 7 presents a typical scatter plot. This plot represents changes in the model output related to the changes in one input parameter [24]. The output is the frequency of floodplain inundation calculated for the cross-section at km

503+560 at the river state 2004-a. The parameter analyzed is the roughness coefficient  $n$  for channel bed in the same cross-section. The horizontal axis represents values of the parameter. The vertical axis represents values of frequency in total admissible range, from 0 to 1. The results are shown as points.

### Discussion

#### Water Stages Frequency

Analysis of the results shows a significant shift of water stages toward the range of higher values, which means that the inundation of floodplains has become more frequent (Fig. 4). For the cross section at Km 503+140, flooding is permanent. The most frequent stages are higher and their frequency has also increased. Moreover, the higher stages are shifted toward the dike crest, which is more visible in the section located at Km 503+560.

The results presented in Tables 1-4 show the permanent increase in the average water levels at each cross-section. The deviation of the stages from the average decreases. The exception is the deviation for the last state 2004-b, meaning that the increase in the roughness related to vegetation growth leads to greater standard deviation.

#### Floodplain Inundation Frequency

The frequency of floodplain inundation also increases in all cross-sections analyzed. In the sections located upstream, at Km 503+560 (Table 1, Fig. 5) and Km 503+380 (Table 2), the influence of the reservoir is negligible. It is clear if one compares the state from 1985-a and that

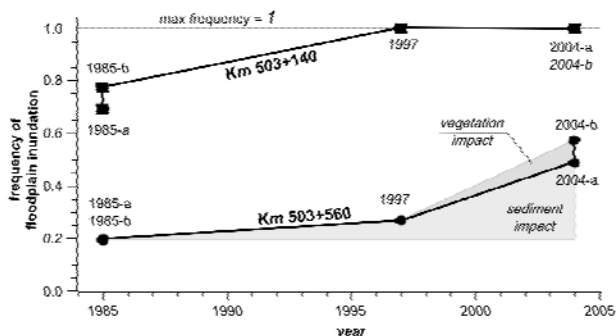


Fig. 5. Simulated frequencies of floodplain inundation for the cross-sections at km 503+560 and at km 503+140.

Table 6. Measures of increase in frequency of floodplain inundation for cross-section in km 503+140.

State	1985-a (first state)	1985-b	1997	2004-a	2004-b (final state)	TOTAL
$FFI_j$	0.692	0.772		1.000		1.000
$FFI_j - FFI_{j-1}$	-	0.080		0.228		0.308
$\Delta FFI_j^{(1)}$	-	26.0%		74.0%		100%
$\Delta FFI_j^{(2)}$	-	11.6%		32.9%		-

from 1985-b in Tables 1 and 2. For the cross sections located lower, at Km 503+140 (Table 3, Fig. 5) and Km 502+800 (Table 4), this element is more important. In these sections maximum flooding ( $= 1.0$ ) was reached in the state from 1997. Then the influence of the vegetation was not observed because of huge sediment accumulation. The degree of sedimentation at sections Km 503+560 (Table 1) and Km 503+380 (Table 2) is not so high, hence the small impact of riparian vegetation. This is the difference between the state from 2004-a and that from 2004-b. However, the impact of the sediment deposition on floodplain inundation was also much greater in the upper sections.

The real importance of the riparian vegetation is visible if the frequency of extreme stages is analyzed. This effect was noticed for the upper sections, at Km 503+560 (Table 1, Fig. 5) and Km 503+380 (Table 2). The vegetation causes an increase in the frequency calculated for higher stages. In Tables 1 and 2 the frequencies of selected stage exceedances are shown. These stages are equal to 0.5 m, 1.0 m, and 1.5 m below the dike crest. The cells corresponding to results different than zero are shaded. The increase in the dike-break risk is obvious. Similar problems were not observed for the lower sections, at Km 503+140 (Fig. 5) and Km 503+800.

### Comparison of Impacts

The examples shown in Tables 5-6 and Fig. 6 confirm the observations from the previous sections of the paper. The effect of reservoir operation was not noted in the cross-section at 503+560. For this location the most important factor was sediment deposition. The vegetation impact was about one third of that caused by sedimentation. The relations are different for the cross-section at 503+140. The vegetation effect was not noted, but the effect of the reservoir operation is comparable with that of sediment deposition.

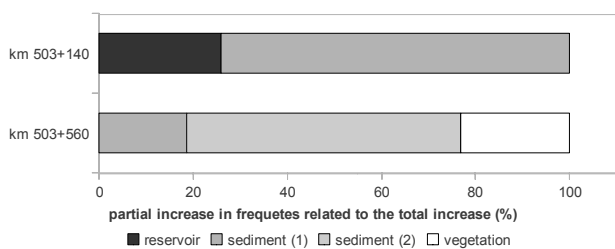


Fig. 6. Increase in frequency related to the total increase  $\Delta FFI_j^{(1)}$  shown for two cross-sections.

These results indicate that the importance of particular impacts depends on the location of a given cross-section. The reservoir operation has small influence upstream. In the cross-sections located downstream, the effect of this process is comparable with that of sediment deposition. On the other hand, the influence of vegetation succession is not detected in the downstream location, though it seems to be an important factor for upstream cross-sections.

In general, the importance of the reservoir operation increases with increasing downstream location of a given cross-section. The reasons are clearly understandable. The cross-section that is nearer the dam is more influenced by the water stages kept in the dam. The influence may be so strong that the effects of the other factors are less visible.

The effect of vegetation increases in upstream cross-sections. This factor is not the most important one for the total increase in flooding frequency, but its impact is pronounced at the most dangerous extreme water stages. Hence, it should not be neglected.

The most important factor at all locations is sediment deposition. This process changes hydraulic conditions in the river, as well as in the floodplains. Its influence is clearly visible in both cross-sections studied.

### Uncertainty of Simulation Results

The results of uncertainty analysis are shown in Table 7, where the values of  $RDF$  and  $RWF$  suggest that inaccuracies in the determination of the roughness coefficients  $n$  do not impact the frequency of floodplain inundation  $FFI$  much. Analysis of Fig. 7 leads to similar conclusions. Intuitively, the arbitrarily chosen roughness coefficient  $n$  is considered the most important source of uncertainty. In fact, the changes in  $n$  at the cross-section for which the flooding frequency is calculated do not much influence the results of calculation. The range of the analyzed frequency,  $RWF$ , is not small, because its relative value is over 10%. However, the  $RDF$  measure equals about 0.22% when the standard deviation is 0.017. This is very small, which is also consistent with the results presented in Fig. 7. In this figure the frequency of flooding inundation  $FFI$  is almost constant along the range of roughness variation.

As shown in Table 7, the changes in the roughness coefficients  $n$  at the other cross-sections have even smaller impact on flooding frequency at the cross-section 503+560. The obvious conclusion is that the impact of  $n$  decreases with the distance from the cross-section. The next observa-

Table 7. Summary of uncertainty assessment for frequency of floodplain inundation in cross-section 503+560.

Parameter	Cross-section		
	513+490	503+560	494+330
$n$	$0.035 \text{ s}\cdot\text{m}^{-1/3}$	$0.040 \text{ s}\cdot\text{m}^{-1/3}$	$0.045 \text{ s}\cdot\text{m}^{-1/3}$
$FFI$	0.485		
$E_f$	0.485	0.484	0.485
$\sigma_f$	0.000	0.017	0.000
$FFI_m$	0.485	0.462	0.485
$FFI_M$	0.485	0.512	0.485
$RDF$	0.02%	0.22%	0.01%
$RWF$	0.03%	10.76%	0.00%

tion is that the impact of  $n$  at the downstream cross-section (km 494+330) is smaller than at the upstream location (km 513+490). The downstream cross-section is under strong influence of reservoir management and the water levels at this site are higher. This factor decreases the influence of roughness coefficient at this location.

It is important to note that the results obtained depend on elements of the methodology and the factors selected for the uncertainty analysis. The whole procedure and the frequency of floodplain inundation seem to be resistant to uncertainty impacts. If other elements are analyzed in the same way, e.g. inundation related to maximum flows, the uncertainty analysis could give different results.

## Conclusions

Changes in the Warta River flooding frequency related to the effect of sediment deposition and riparian vegetation growth were analyzed by the method combining data collection, hydrodynamic simulation and frequency analysis. The analyses show that an increase in bottom elevations

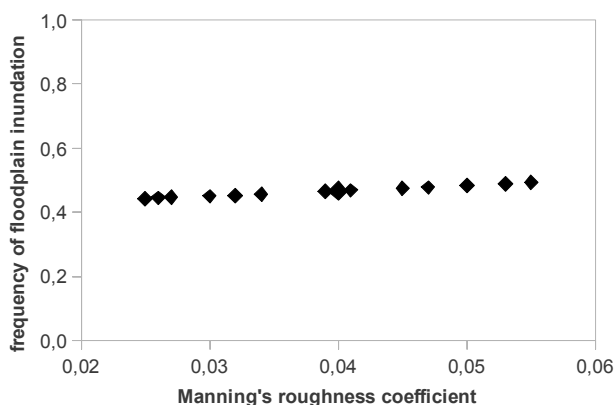


Fig. 7. Changes in floodplain inundation frequency for the cross-sections at km 503+560 in state 2004-a with changes in Manning's roughness coefficient in channel zone at the same cross-section.

from state to state causes an increase in the average water stages and flood frequency. The range of the most common water stages is narrowed, as follows from the changes in standard deviations. Increase in floodplain roughness causes a widening of the water stage ranges, as indicated by greater standard deviation for the data from 2004-b than for the data from 2004-a. The frequency of floodplain inundation is permanently increasing. For some bottom states, the maximum admissible frequency (= 1.0) is reached mainly as a result of sediment deposition. However, for some specific bottom states the reservoir operation, as well as riparian vegetation growth, may be significant. The influence of riparian vegetation becomes important for higher water stages and the vegetation development can be crucial for increasing the dike breach risk.

The analyses show that sediment accumulation is the main factor responsible for permanent increase in flooding frequency. The obvious conclusion for river management seems to be that river regulation with removal of sediments is the proper way to restrain adverse conditions. Such a solution increases the channel capacity, decreases the frequency of flooding inundation and improves the overall condition for land use. River restoration also decreases the elevation of extreme water stages responsible for flood risk, but this effect is achieved indirectly through a decrease in the total flooding frequency. Direct improvement in the hydrological conditions and related dike breach risk may be achieved by removal of vegetation. According to the above comparative analysis, the appearance of vegetation is the most important cause of increase of the extreme water states.

The difference between river restoration and removal of vegetation is important if there are conflicting expectations for the river functions and management, e.g. flood protection, and ecosystem conservation. It is clearly seen that river restoration is good for land use, less good for flood protection, and not a good method for ecosystem conservation. On the other hand, reasonable removal of vegetation may decrease flood risk and help conserve the present ecosystem features as much as possible without harm in any other ways of ecosystem functioning. However, the latter method has a low impact on improvements of land use. The choice between river restoration and vegetation removal is not obvious and should be made carefully.

The presented procedure consisting of data collection, hydrodynamic simulation, and frequency analysis seems to be a good diagnostic tool. It enables assessment of current river state against a background of historical channel and floodplain conditions. The methodology may be extended for prognostic applications. However, the sediment transport model and proper model for bush growth and vegetation succession should then be applied. The application of such models would need a proper selection of inflow scenarios and reliable information on the directives and rules of reservoir management.

An important factor in diagnostic and prognostic applications is the uncertainty of determination of the model parameters. The results obtained suggest that the methodology presented is resistant to uncertainties. This property follows from a robust construction of the simulation procedure

and selection of measures for the assessment of system state. All these features permit extension of the method for application for river management. The methodology completed with sediment transport model, vegetation growth model and detail uncertainty analysis may be used as a typical “*what-if*” tool. The results presented show that further research in this area is promising.

### Acknowledgements

This work is a part of a scientific grant, “Initial sedimentation part in small lowland reservoirs: modelling and analysis of functionality,” funded by the National Science Centre in Poland, project No. N N305 296740.

### References

1. KEELAND B.D., CONNER W.H., SHARITZ R.R. A comparison of wetland tree growth response to hydrologic regime in Louisiana and South Carolina. *Forest Ecology and Management*, **90**, 237, **1997**.
2. SURTEVANT B.R. A model of wetland vegetation dynamics in simulated beaver impoundments, *Ecological Modeling*, **112**, 195, **1998**.
3. STROMBERG J.C. Restoration of riparian vegetation in the south-western United States: importance of flow regimes and fluvial dynamism. *Journal of Arid Environments*, **49**, 17, **2001**.
4. NILSSON C., SVEDMARK M. Basic principles and ecological consequences of changing water regimes: riparian plant communities. *Environmental Management*, **30**, (4), 468, **2002**.
5. PETTS G.E., GURNELL A.M. Dams and geomorphology: research progress and future directions. *Geomorphology*, **71**, 27, **2005**.
6. MAINGI J.K., MARSH S.E. Quantifying hydrologic impacts following dam construction along the Tana River. Kenya. *Journal of Arid Environments*, **50**, 53, **2002**.
7. MAGILLIGAN F.J., NISLOW K.H. Changes in hydrologic regime by dams. *Geomorphology*, **71**, 61, **2005**.
8. MARSTON R.A., MILLS J.D., WRAZIEN D.R., BASSETT B., SPLINTER D.K. Effects of Jackson Lake Dam on the Snake River and its floodplain, Grand Teton National Park, Wyoming, USA. *Geomorphology*, **71**, 79, **2005**.
9. MUMBA M., THOMPSON J.R. Hydrological and ecological impacts of dams on the Kafue Flats floodplain system, southern Zambia. *Physics and Chemistry of the Earth*, **30**, 442, **2005**.
10. PINTER N., HEINE R.A. Hydrodynamic and morphodynamic response to river engineering documented by fixed-discharge analysis, Lower Missouri River, USA. *Journal of Hydrology*, **302**, 70, **2005**.
11. KING S.L., ALLEN J.A., MCCOY J.W. Long-term effects of a lock and dam and green tree reservoir management on a bottomland hardwood forest. *Forest Ecology and Management*, **112**, 213, **1998**.
12. WELLMAYER J.L., SLATTERY M.C., PHILLIPS J.D. Quantifying downstream impacts of impoundment on flow regime and channel planform, lower Trinity River, Texas. *Geomorphology*, **69**, 1, **2005**.
13. KITE G. Modelling the Mekong: Hydrological simulation for environmental impact studies. *Journal of Hydrology*, **253**, 1, **2001**.
14. WICHER-DYSARZ J., PRZEDWOJSKI B. Modeling of sediment accumulation in the inlet part of Jeziorsko reservoir, *Annual Reviews of Agricultural University of Poznan*, **26**, 483, **2005**.
15. KLOPSTRA D., BARNEVELD H.J., VAN NOORTWIJK J.M., VAN VELZEN E.H. Analytical model for hydraulic roughness of submerged vegetation. The 27<sup>th</sup> Congress of the International Association for Hydraulic Research, Proceedings of Theme A, Managing Water: Coping with Scarcity and Abundance, San Francisco, California, **1997**.
16. WALCZAK N., PRZEDWOJSKI B. Determination of resistance coefficients for floodplains of the Warta river upstream of the Jeziorsko reservoir, *Annals of Agricultural University of Poznan*, **2005** [In Polish].
17. BRUNNER G.W. HEC-RAS, River Analysis System hydraulic reference manual, computer program documentation. Davis, CA.: US Army Corps of Engineers, Hydrologic Engineering Center, **2002**.
18. LIGGETT M.B., CUNGE J.A. Numerical methods of solution of the unsteady flow equations, in Mahmood and Yevjevich. In: MAHMOOD K., YEVJEVICH V. (Eds.). *Unsteady flow in open channels*. Fort Collins, Colorado: Water Resources Publications, **1975**.
19. ABBOTT M.B. *Computational Hydraulics, Elements of the Theory of Free Surface Flows*. London: Pitman, **1979**.
20. CUNGE J.A., HOLLY F.M.J.R., VERVEJ A. *Practical aspects of computational river hydraulics*, Pitman Advanced Publishing Program, **1988**.
21. BARKAU R.L. Simulation of the July 1981 flood along Salt River, Report for CE695BV, Special Problems in Hydraulics. Fort Collins, CO.: Department of Civil Engineering, Colorado State University, **1982**.
22. ARMANINI A., RIGHETTI M., GRISSENTI P. Direct measurement of vegetation resistance in prototype scale. *Journal of Hydraulic Engineering*, **43**, (5), 481, **2005**.
23. CHOW V.T., MAIDMENT D.R., MAYS L.W. *Applied Hydrology*. McGraw-Hill International Editions, Civil Engineering Series, McGraw-Hill Book Company, **1988**.
24. SALTELLI A., RATTO M., ANDRES T., CAMPOLONGO F., CARIBONI J., GATELLI D., SAISANA M., TARANTOLA S. *Global Sensitivity Analysis. The Primer*. John Wiley & Sons Ltd., **2008**.
25. HALL J.W., BOYCE S.A., WANG Y., DAWSON R.J., TARANTOLA S., SALTELLI A. Sensitivity analysis for hydraulic models. *Journal of Hydraulic Engineering*, **135**, (11), **2009**.
26. CHOW V.T. *Open Channel Hydraulics*, McGraw-Hill College, **1959**.

